MATERIALS SCIENCE

Skyrmion lattice structural transition in MnSi

Taro Nakajima,[1]* Hiroshi Oike,[1] Akiko Kikkawa,[1] Elliot P. Gilbert,[2] Norman Booth,[2] Kazuhisa Kakurai,[1,3†] Yasujiro Taguchi,[1] Yoshinori Tokura,[1,4] Fumitaka Kagawa,[1] Taka-hisa Arima[1,5]

Magnetic skyrmions exhibit particle-like properties owing to the topology of their swirling spin texture, providing opportunities to study crystallization of topological particles. However, they mostly end up with a triangular lattice, and thus, the packing degree of freedom in the skyrmion particles has been overlooked so far. We report a structural transition of the skyrmion lattice in MnSi. By use of small-angle neutron scattering, we explore a metastable skyrmion state spreading over a wide temperature and magnetic field region, after thermal quenching. The quenched skyrmions undergo a triangular-to-square lattice transition with decreasing magnetic field at low temperatures. Our study suggests that various skyrmion lattices can emerge at low temperatures, where the skyrmions exhibit distinct topological nature and high sensitivity to the local magnetic anisotropy arising from the underlying chemical lattice.

INTRODUCTION

When particles condense to form a crystal, many possibilities arise regarding their configurations, which are often determined by the symmetry of the constituents. For instance, noble gases, fullerene (at room temperature) (*1*, *2*), and group 1B elements (Cu, Ag, and Au) crystallize in face-centered cubic structures because these particles can effectively behave as spheres. In two-dimensional systems, triangular lattices show up as a consequence of the close packing of circular objects, as observed in vortex lattices in type II superconductors (*3*) and Bose-Einstein condensates of alkali atoms (*4*). By contrast, silicon (Si) has a diamond structure, which is not close packing, reflecting four covalent sp^3 bonds from the central atom. These observations remind us of a perspective on crystallization of particles; as some anisotropy is introduced into the system, the density becomes less important, and instead, the bonding (that is, how the two particles connect with each other) becomes more important.

Here, we apply this perspective to the magnetic skyrmion, which is a novel type of topologically protected particle-like spin texture (*5*–*7*). To introduce the anisotropy in the skyrmion system, we focus on coupling between the spins and the underlying chemical lattice, which is supposed to be more effective at low temperatures, in analogy with vortex lattices in anisotropic superconductors (*8*–*10*). However, in a bulk crystal of the archetypal skyrmion compound MnSi (*11*), which has a cubic crystal structure, the skyrmions appear only in a narrow temperature and magnetic field region near the magnetic transition temperature (for a typical phase diagram, see Fig. 1A) (*11*–*14*); the skyrmion state is thus easily transformed into a single-*q* conical magnetic order due to strong thermal fluctuations, before changing the lattice symmetry. Although the skyrmions become more stable in thin-film samples (*12*, *15*–*17*), the effect of the magnetic anisotropy from the chemical lattice is relatively weak as compared with other effects, such as the long-ranged magnetic dipolar interaction, which is significant, especially in the thin-plate samples. Another strategy to stabilize the skyrmion state is to introduce uniaxial anisotropy, as was predicted in previous theoretical studies (*18*–*21*). This situation has been experimentally realized mostly in epitaxial film samples thus far (*21*). However, the thermodynamic stability and packing degree of freedom of the skyrmions have not been investigated in these systems.

To overcome this problem, we use the "metastable" skyrmion state. Since the pioneering studies on helimagnets (*22*) and magnetic skyrmions (*5*), a number of theoretical studies have proposed that the skyrmion state appears not only as a thermoequilibrium state but also as a metastable state (*18*–*20*). It has been recently revealed that the metastable skyrmion state is realized in a bulk crystal of MnSi by quenching the thermodynamically stable skyrmion lattice (SkL) to low temperatures (*23*). The quenched skyrmion state is stabilized in a much wider magnetic field range at low temperatures, as compared to the equilibrium SkL state (*23*). This demonstrates that each skyrmion particle becomes more robust at low temperatures, implying that the topological nature of the spin texture becomes more pronounced as the thermal fluctuations are reduced. Here, we explore the quenched skyrmion state by small-angle neutron scattering (SANS) measurements on a single crystal of MnSi to investigate the packing degree of freedom in magnetic skyrmion particles.

RESULTS AND DISCUSSION

Before going into the quenched skyrmion state, we measured SANS patterns under equilibrium conditions in two configurations, specifically the $H \parallel \boldsymbol{k}_i$ and $H \perp \boldsymbol{k}_i$ configurations, where H and $\boldsymbol{k}_i$ are the external magnetic field and wave vector of the incident neutrons, respectively (Fig. 1B). The direction of the magnetic field was set to be parallel to the [001] direction of the crystal. In the equilibrium SkL phase at 28 K and 0.2 T, we observed a hexagonal diffraction pattern in the $H \parallel \boldsymbol{k}_i$ configuration (Fig. 1C), which is a hallmark of the triangular SkL (*11*). As the temperature decreases, the SkL phase turns into a conical phase with the magnetic modulation wave vector parallel to H. Accordingly, the magnetic reflections were observed only in the $H \perp \boldsymbol{k}_i$ configuration in the conical phase, as shown in Fig. 1 (D and G).

To obtain the quenched skyrmion state, we used the electric current pulse method established in the previous study of Oike *et al.* (*23*).

[1]RIKEN Center for Emergent Matter Science, Saitama 351-0198, Japan. [2]Australian Centre for Neutron Scattering, Australian Nuclear Science and Technology Organisation, New South Wales, Australia. [3]Quantum Beam Science Center, Japan Atomic Energy Agency, Tokai, Ibaraki 319-1195, Japan. [4]Department of Applied Physics and Quantum-Phase Electronics Center, University of Tokyo, Tokyo 113-8656, Japan. [5]Department of Advanced Materials Science, University of Tokyo, Kashiwa 277-8561, Japan.
*Corresponding author. Email: taro.nakajima@riken.jp
†Present address: Research Center for Neutron Science and Technology, Comprehensive Research Organization for Science and Society, Tokai, Ibaraki 319-1106, Japan.

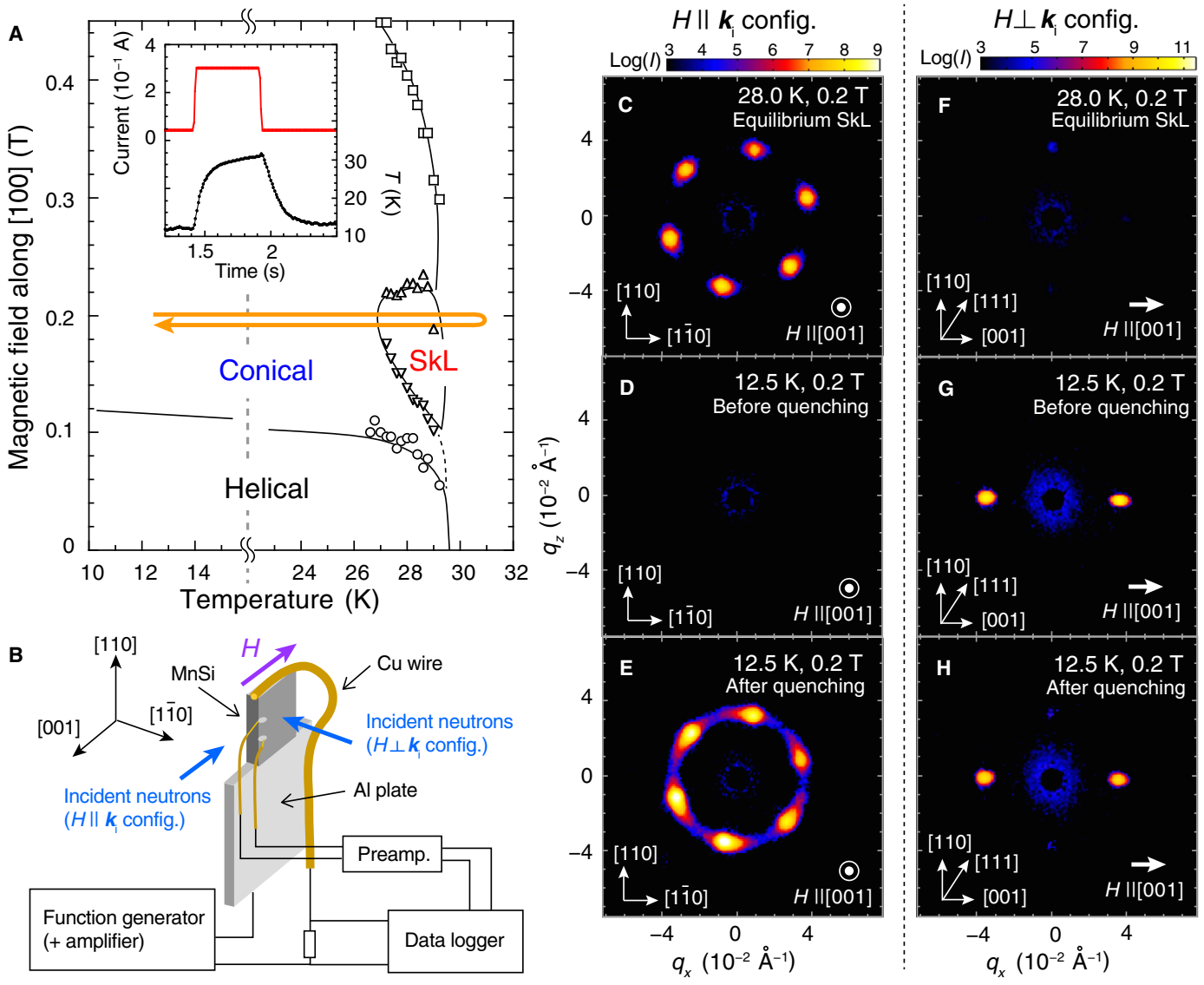

Fig. 1. SANS measurements on equilibrium magnetic phases and quenched SkL state under a magnetic field of 0.2 T. (**A**) *H-T* magnetic phase diagram of MnSi. The open symbols denote phase boundaries between helical, conical, SkL, and field-induced ferromagnetic phases determined by resistivity measurements using the identical sample used in the SANS measurements. Inset: Typical time profiles of an electric current pulse and the resulting temperature change. (**B**) Schematic showing the experimental setup, orientation of the crystal, and directions of neutron beam and magnetic field. (**C** to **E**) SANS patterns measured in the $H \parallel \boldsymbol{k}_i$ configuration (C) in the equilibrium SkL phase, at 12.5 K and 0.2 T before applying the current pulse (D), and after the application of the pulse (E). (**F** to **H**) Corresponding SANS patterns measured in the $H \perp \boldsymbol{k}_i$ configuration.

As shown in Fig. 1B, four electrodes were attached on the sample in the same manner as standard resistivity measurements. We applied a current pulse with a typical height and width of 300 mA and 0.5 s, respectively, at 12.5 K and 0.2 T. By measuring the resistivity during the current pulse application, we deduced the sample temperature as a function of time (Fig. 1A, inset); the sample was heated to the paramagnetic phase within 0.5 s and then rapidly back to 12.5 K, passing through the equilibrium SkL phase lying between 29 and 27 K (Fig. 1A) with a cooling speed of approximately 100 K/s. After the current pulse application, we observed a hexagonal diffraction pattern in the $H \parallel \boldsymbol{k}_i$ configuration (Fig. 1E), unequivocally showing that the quenched skyrmions have the triangular lattice form similar to that of the equilibrium SkL phase. We also note that the conical phase also survived after the quenching, as shown in Fig. 1H. By measuring the cooling rate dependence of the SANS patterns in detail, we conclude that the volume fraction of the quenched SkL was approximately 50% in the present experiment (see the Supplementary Materials).

Having obtained the quenched triangular SkL, we then investigated its magnetic field dependence at the lowest temperature, 1.5 K, where the particle nature of the skyrmion is supposed to be well pronounced; specifically, at low temperatures, each skyrmion tends to behave as a topological defect, which cannot be destroyed without thermal fluctuation. By changing the magnetic field in this extreme condition, we expect a new form of SkL to appear that reflects the competition among different interactions, specifically symmetric and asymmetric exchange interactions, magnetic anisotropy, Zeeman interaction, among

others. Figure 2A shows magnetic field dependence of the integrated intensity of the magnetic reflections measured in the $H \parallel k_i$ configuration. When the magnetic field was increased from 0.2 T, the integrated intensity reduced to zero at around 0.45 T without changing the hexagonal symmetry in the SANS pattern. In contrast, when the magnetic field decreased, a fourfold SANS pattern emerged in the $H \parallel k_i$ configuration (Fig. 2K), right after the integrated intensity sharply dropped at around 0.1 T. This marked change in symmetry is also clearly seen in the azimuthal angle (Ψ) profile (as shown in Fig. 2, E to G): At 0.2 T, six peaks were observed at 60° intervals (Fig. 2E); as the magnetic field decreased, these peaks became rather broad (Fig. 2F), and thus, a ring-like diffraction pattern was observed at 0.08 T (as shown in Fig. 2J); finally, four sharp peaks appeared along the ⟨110⟩ directions at 0 T (Fig. 2G). We also traced field dependence of the residual conical order on the $H \perp k_i$ configuration. At 0.2 T, two reflections were observed along the direction of the magnetic field (Fig. 2M). As the magnetic field was decreased, the conical reflections deviated from the [001] direction and ended up with four reflections along the ⟨111⟩ directions in zero field (as shown in Fig. 2, M and O) (see also the Supplementary Materials). These reflections are ascribed to helical magnetic orders with magnetic modulation wave vectors of (*q*,*q*,*q*) and their equivalents and are different in origin from the fourfold diffraction pattern. From these results, we conclude that the quenched skyrmions change their lattice form from triangular to square lattice, reflecting subtle magnetic anisotropy on the (001) plane of the underlying chemical lattice, which has cubic symmetry.

Here, we emphasize that a nonzero Hall voltage was detected in zero field at low temperatures after quenching (Fig. 2D), even though a coexistence of the triangular SkL is not discernible in the SANS pattern at 0 T (Fig. 2G). This strongly suggests that the square lattice skyrmion state contains topological windings that induce an unconventional Hall effect due to scalar spin chirality, which is known as the topological Hall effect (*24*). However, further studies (particularly real-space observation of the zero-field SkL state) will be necessary to thoroughly exclude the possibility that the fourfold diffraction pattern would be merely due to a multidomain state of single-*q* helical magnetic orders or a nontopological 2*q* state.

We also note that the sixfold diffraction pattern was retrieved when a magnetic field of 0.2 T was applied after reaching the square SkL state at 1.5 K (Fig. 2H), indicating that the skyrmion particles were rearranged again to form the triangular lattice. However, the integrated intensity in

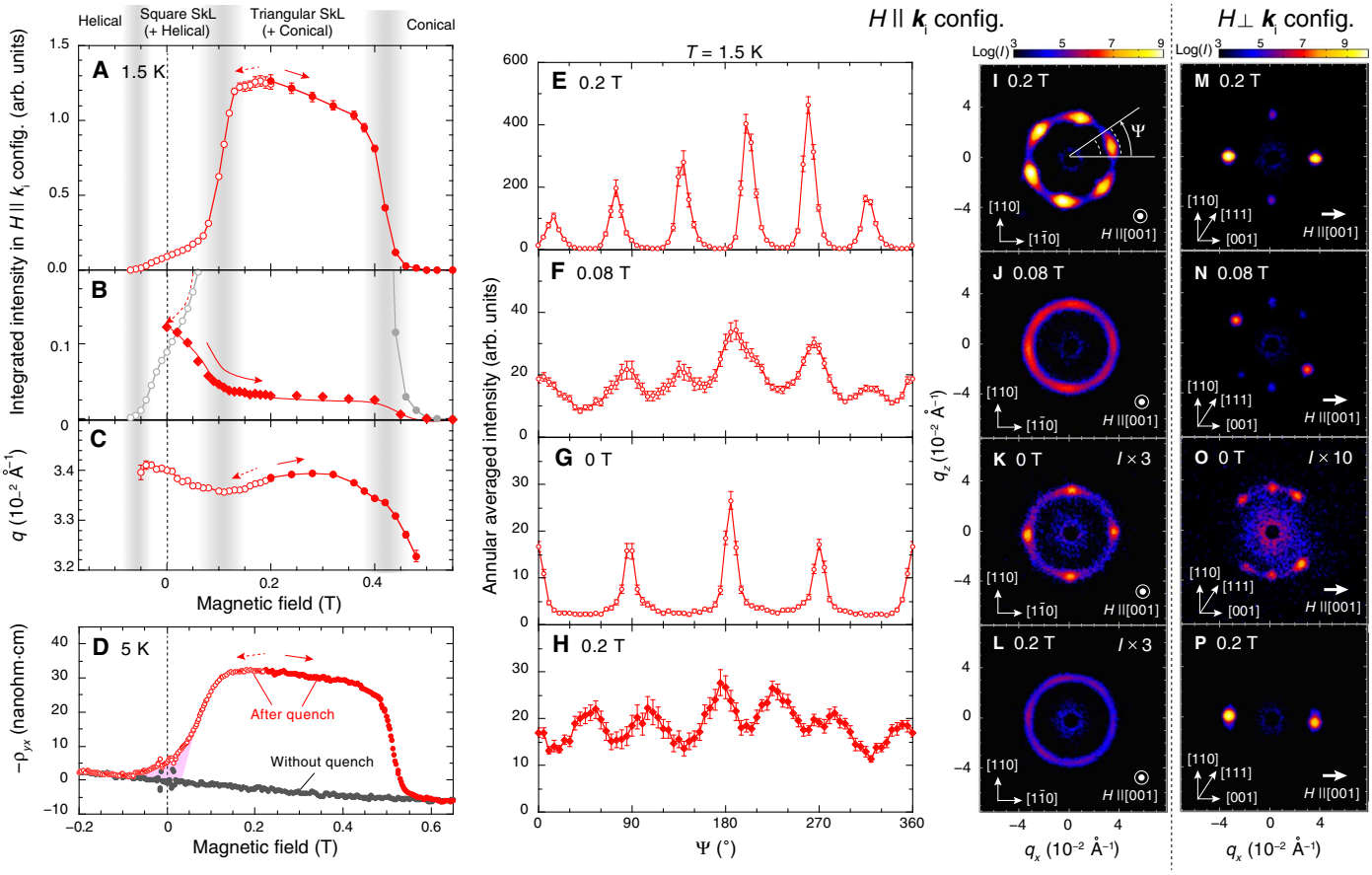

Fig. 2. Magnetic field induced transitions in the lowest temperature (1.5 K) after quenching. (**A**) Magnetic field dependence of integrated intensity of the magnetic reflections measured in the $H \parallel k_i$ configuration after quenching at 0.2 T with increasing and decreasing fields and (**B**) measured with increasing magnetic field after reaching the square SkL state in zero field. (**C**) Field dependence of average values of peak position in *q* measured in the $H \parallel k_i$ configuration at 1.5 K. Filled and open symbols denote data measured with increasing and decreasing field, respectively. Gray data points in (B) are the data shown in (A). (**D**) Hall resistivity data redrawn from fig. S3a in the Supplementary Materials of the study by Oike *et al.* (*23*). Expected square SkL contribution in Hall resistivity is highlighted in pink. Slight discrepancies in transition fields are due to differences in temperature and demagnetizing effect. (**E** to **H**) Azimuthal angle profiles of the annular-averaged intensities measured at (E) 0.2 T, (F) 0.08 T, and (G) 0 T with decreasing field and at (H) 0.2 T with increasing field from 0 T. (**I** to **P**) The SANS patterns measured in the $H \parallel k_i$ and $H \perp k_i$ configurations at the selected magnetic fields. In (K), (L), and (O), the intensities (*I*) are multiplied by factors of 3, 3, and 10, respectively, to enhance clarity.

the $H \parallel \boldsymbol{k}_i$ configuration was further decreased (as shown in Fig. 2B), implying that some parts of the skyrmions were transformed into the helical or conical magnetic orders when crossing the boundary between the square and triangular SkL states. The partial collapse of the metastable skyrmions is also supposed to occur when the triangular SkL transforms into the square lattice with decreasing field. To estimate the volume fraction of the square SkL in zero magnetic field, it would be necessary to measure the magnetic reflections from the remainder of the fractions, that is, the helical magnetic order, which has four domains corresponding to wave vectors of (*q*,*q*,*q*) and its equivalents, although two of them were not accessible in the present experimental configuration.

By measuring the magnetic field and temperature dependence of the SANS patterns after quenching, we investigated the stability of the triangular and square SkLs on the *H*-*T* magnetic phase diagram (see the Supplementary Materials for details). The results are summarized in Fig. 3; the metastable triangular SkL was observed in a wide temperature and magnetic field range, whereas the square SkL appears only at low temperatures and low magnetic fields. The overall area where the metastable SkLs were observed agrees with that identified from the previous Hall resistivity measurements (*23*).

The marked change in lattice symmetry implies that some anisotropy developed in the particles and interactions between them. Although the anisotropy within the skyrmion particles cannot be directly resolved from the present SANS measurements, it is reasonable to consider that the spin textures of the skyrmions change with decreasing field; specifically, the number of magnetic moments pointing in lateral directions should increase with decreasing magnetic field because of the reduction of net magnetization. The increased lateral components of the local magnetic moments would tend to be more susceptible to the subtle magnetic anisotropy on the (001) plane of the chemical lattice and could lead to the square lattice skyrmion state. This scenario can also be accounted for as follows. The intervening regions between the skyrmions, where the magnetic moments were parallel to the external magnetic field (see Fig. 4A), should be squeezed with decreasing field.

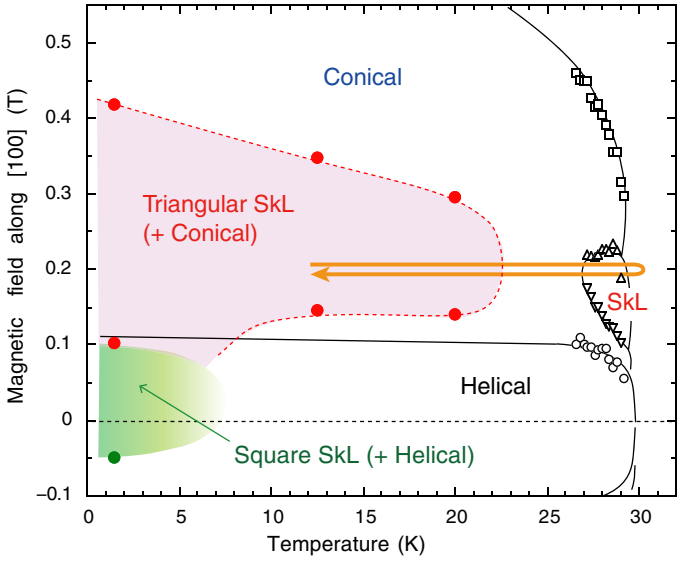

Fig. 3. Metastable state diagram mapped on the *H*-*T* magnetic phase diagram. Metastable state diagram mapped on the *H*-*T* magnetic phase diagram. The filled circles denote the boundaries between the metastable triangular SkL, square SkL, and (equilibrium) conical and helical magnetic states.

As a result, the skyrmions could partly overlap each other, being rearranged to find a more stable lattice form. Here, the magnitude of the *q* vector remains nearly constant through the transition from the triangular to the square SkL (Fig. 2C), indicating that the core-to-core distance of the spin-swirling objects becomes shorter in the square lattice than in the triangular lattice (Fig. 4B). A recent theoretical study by Lin *et al.* (*25*) suggests that the overlap between neighboring skyrmions can trigger a transition to a square lattice of fractionalized skyrmions. They numerically studied evolutions of spin textures in a two-dimensional spin system with ferromagnetic exchange interaction, Dzyaloshinskii-Moriya interaction, and easy-plane anisotropy. Their calculation successfully reproduced the triangular SkL under a magnetic field, when the easy-plane anisotropy is sufficiently smaller than the other interactions. As the easy-plane anisotropy increases, the intervening regions with upward magnetic moments are reduced because the magnetic moments lying in the plane are favored by the anisotropy. This leads to the overlap of the skyrmions, and finally, the triangular SkL transforms into a square lattice of (fractionalized) skyrmions. This situation is qualitatively similar to the quenched skyrmion state in zero magnetic field; instead of increasing the easy-plane anisotropy, we reduced the external magnetic field in the quenched SkL state at the lowest temperature so that the number of upward moments was decreased to reduce the net

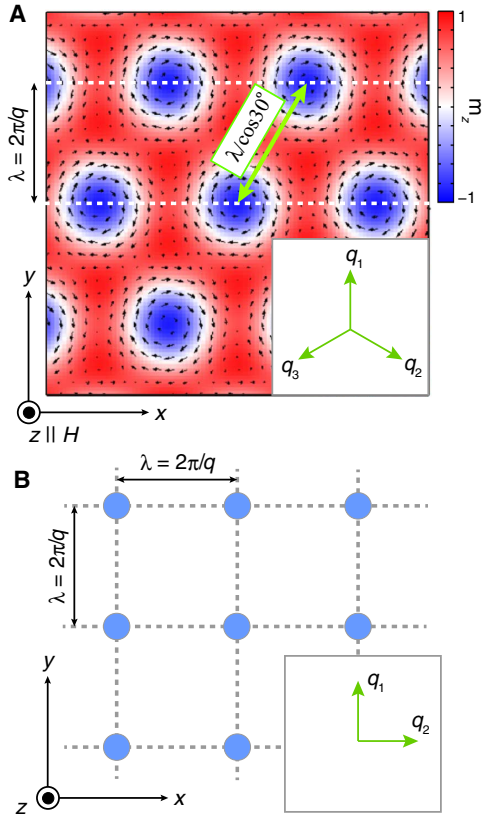

Fig. 4. Triangular SkL and square lattice arrangements of particles with the same modulation period λ. (**A**) The triangular SkL described by superposition of three screw magnetic modulations of $\boldsymbol{q}_1$, $\boldsymbol{q}_2$, and $\boldsymbol{q}_3$ ($|\boldsymbol{q}_i| = 2\pi/\lambda$, i = 1 to 3) shown in its inset and a uniform magnetization component along the *z* direction. Colors and arrows denote out-of-plane and in-plane components of the magnetic moments, respectively. (**B**) Schematic showing square lattice arrangements of particles characterized by two wave vectors of $\boldsymbol{q}_1$ and $\boldsymbol{q}_2$ ($|\boldsymbol{q}_i| = 2\pi/\lambda$, i = 1, 2) shown in its inset.

magnetization. Although the theoretical study by Lin *et al.* (*25*) focused on a phase diagram of the lowest-temperature equilibrium states in the two-dimensional model, we suggest that a balance between Zeeman energy and magnetic anisotropy is critical to understand the SkL structural transition in the metastable states in three-dimensional materials.

Here, a fourfold magnetic diffraction pattern was also observed in another skyrmionic compound, $Co_8Zn_8Mn_4$ (*26*). Our results suggest that the triangular-to-square lattice transition is more general of the skyrmion systems and that the square SkL state has topological windings. Also, note that the length of the q vector in $Co_8Zn_8Mn_4$ strongly depends on temperature (*26*), whereas that in MnSi does not. This observation suggests that the temperature variation of q is not essential for the formation of the square SkL. In the square SkL state of $Co_8Zn_8Mn_4$, the directions of the q vectors are confined to be parallel to the ⟨100⟩ directions, which also coincides with one of the q vectors in the triangular SkL phase. These results imply that the magnetocrystalline anisotropy plays a crucial role in the SkL structural transitions in these compounds.

From another point of view, we found similarities between the observed square SkL state and the "partial order" state, which was discovered as a pressure-induced state in MnSi (*27*) and is supposed to have a topologically nontrivial spin texture (*28*, *29*). Both the magnetic states have magnetic reflections peaking along the ⟨110⟩ directions and appear in zero magnetic field at low temperatures. These similarities imply that there is a common topology in the spin textures of these states.

Our results show the possibility that various forms of SkLs, which are unobservable in the thermoequilibrium phase diagram, appear at low temperatures and low magnetic fields, where the skyrmions exhibit both a distinct topological nature and high sensitivity to anisotropic perturbations arising from the underlying chemical lattice. Also, vortices in a rotating two-component Bose-Einstein condensate, which are also topological defects with packing degree of freedom, exhibit a triangular-to-square lattice structural transition (*30*, *31*). We thus suggest that the quenched metastable skyrmion state will be a fertile ground to study crystallization of topological particles.

MATERIALS AND METHODS

A single crystal of MnSi was grown by the Czochralski method and was cut into a plate shape with dimensions of 3 mm × 3 mm × 0.5 mm. The widest surfaces are normal to the $[1\bar{1}0]$ direction of the crystal with the other surfaces normal to the [001] and [110] directions (as shown in Fig. 1B). A Cu wire of 0.5 mm diameter and an Al plate were attached on the [110] surface with silver paste and were used for current leads. Au wires for the voltage probe were attached on the $[1\bar{1}0]$ plane with indium solder and silver paste. After checking the orientation of the crystal using an x-ray Laue backscattering diffractometer, the sample with the electrodes was mounted into a cylinder-shaped sample holder. Before the SANS measurements, we measured the resistivity of this sample in zero magnetic field and under a magnetic field parallel to the [001] direction. The residual resistivity ratio in zero magnetic field was approximately 35. From the field dependence of the resistivity, we determined the thermoequilibrium magnetic phase diagram in the same manner as that done by Oike *et al.* (*23*).

The SANS measurements were conducted at the QUOKKA instrument at the Australian Nuclear Science and Technology Organisation. We attached Cd plates with a hole of 3 mm diameter on the sample holder to reduce the intensity contribution from nonsample scattering. The sample holder was loaded into a horizontal field superconducting magnet (Spectromag, Oxford Instruments). The direction of the magnetic field was parallel to the [001] direction. The SANS patterns were measured in two different configurations, specifically the $H \parallel \boldsymbol{k}_i$ and $H \perp \boldsymbol{k}_i$ configurations (Fig. 1B). The wavelength of the incident neutron was fixed at 5 Å with 10% resolution, the source-to-sample distance was 11.9 m, and the sample-to-detector distance was 8.1 m using a source aperture diameter of 50 mm. All the SANS patterns were measured without rotating the sample. Typical measuring time for a SANS pattern was about 300 s. For all the observed SANS patterns, we performed subtraction of the background signals, which were measured at 20 K in zero field and at 1.5 K under a magnetic field of 1 T for the data measured in the $H \parallel \boldsymbol{k}_i$ and $H \perp \boldsymbol{k}_i$ configurations, respectively. In both the background measurements, no magnetic reflections were observed on the scattering plane. The sensitivity of the area detector was also corrected. We also performed in situ resistivity measurements using the same instruments used by Oike *et al.* (*23*). As described in the main text, we measured the resistivity of the sample during the current pulse application to deduce the time profile of the temperature.

SUPPLEMENTARY MATERIALS

Supplementary material for this article is available at http://advances.sciencemag.org/cgi/content/full/3/6/e1602562/DC1

Cooling rate dependence of the volume fraction of the quenched SkL state

Azimuthal angle profiles measured in the $H \perp \boldsymbol{k}_i$ configuration

Magnetic field and temperature dependence of the quenched SkL states

fig. S1. Cooling rate dependence of the integrated intensities corresponding to the SkL and conical orders.

fig. S2. Field dependence of azimuthal angle profile measured in the $H \perp \boldsymbol{k}_i$ configuration.

fig. S3. Magnetic field and temperature dependence of the metastable SkLs.

Reference (*32*)

REFERENCES AND NOTES

1. R. M. Fleming, T. Siegrist, P. M. Marsh, B. Hessen, A. R. Kortan, D. W. Murphy, R. C. Haddon, R. Tycko, G. Dabbagh, A. M. Mujsce, M. L. Kaplan, S. M. Zahurak, Diffraction symmetry in crystalline, close-packed C_{60}. *MRS Proc.* **206**, 691 (1990).
2. P. A. Heiney, J. E. Fischer, A. R. McGhie, W. J. Romanow, A. M. Denenstein, J. P. McCauley Jr., A. B. Smith, D. E. Cox, Orientational ordering transition in solid C_{60}. *Phys. Rev. Lett.* **66**, 2911 (1991).
3. A. A. Abrikosov, On the magnetic properties of superconductors of the second group. *Sov. Phys. JETP* **5**, 1174–1182 (1957).
4. J. R. Abo-Shaeer, C. Raman, J. M. Vogels, W. Ketterle, Observation of vortex lattices in Bose-Einstein condensates. *Science* **292**, 476–479 (2001).
5. A. N. Bogdanov, D. A. Yablonskii, Thermodynamically stable "vortices" in magnetically ordered crystals. The mixed state of magnets. *Zh. Eksp. Teor. Fiz.* **95**, 178–182 (1989).
6. U. K. Roszler, A. N. Bogdanov, C. Pfleiderer, Spontaneous skyrmion ground states in magnetic metals. *Nature* **442**, 797–801 (2006)
7. N. Nagaosa, Y. Tokura, Topological properties and dynamics of magnetic skyrmions. *Nat. Nanotechnol.* **8**, 899–911 (2013).
8. G. J. Dolan, F. Holtzberg, C. Feild, T. R. Dinger, Anisotropic vortex structure in $Y_1Ba_2Cu_3O_7$. *Phys. Rev. Lett.* **62**, 2184–2187 (1989).
9. Y. De Wilde, M. Iavarone, U. Welp, V. Metlushko, A. E. Koshelev, I. Aranson, G. W. Crabtree, P. C. Canfield, Scanning tunneling microscopy observation of a square Abrikosov lattice in $LuNi_2B_2C$. *Phys. Rev. Lett.* **78**, 4273–4276 (1997).
10. R. Gilardi, J. Mesot, A. Drew, U. Divakar, S. L. Lee, E. M. Forgan, O. Zaharko, K. Conder, V. K. Aswal, C. D. Dewhurst, R. Cubitt, N. Momono, M. Oda, Direct evidence for an intrinsic square vortex lattice in the overdoped high-T_c superconductor $La_{1.83}Sr_{0.17}CuO_{4+\delta}$. *Phys. Rev. Lett.* **88**, 217003 (2002).
11. S. Mühlbauer, B. Binz, F. Jonietz, C. Pfleiderer, A. Rosch, A. Neubauer, R. Georgii, P. Böni, Skyrmion lattice in a chiral magnet. *Science* **323**, 915–919 (2009).
12. S. Seki, X. Z. Yu, S. Ishiwata, Y. Tokura, Observation of skyrmions in a multiferroic material. *Science* **336**, 198–201 (2012).
13. Y. Tokunaga, X. Z. Yu, J. S. White, H. M. Rønnow, D. Morikawa, Y. Taguchi, Y. Tokura, A new class of chiral materials hosting magnetic skyrmions beyond room temperature. *Nat. Commun.* **6**, 7638 (2015).

14. I. Kézsmárki, S. Bordács, P. Milde, E. Neuber, L. M. Eng, J. S. White, H. M. Rønnow, C. D. Dewhurst, M. Mochizuki, K. Yanai, H. Nakamura, D. Ehlers, V. Tsurkan, A. Loidl, Néel-type skyrmion lattice with confined orientation in the polar magnetic semiconductor GaV_4S_8. *Nat. Mater.* **14**, 1116–1122 (2015).
15. X. Z. Yu, Y. Onose, N. Kanazawa, J. H. Park, J. H. Han, Y. Matsui, N. Nagaosa, Y. Tokura, Real-space observation of a two-dimensional skyrmion crystal. *Nature* **465**, 901–904 (2010).
16. X. Z. Yu, N. Kanazawa, Y. Onose, K. Kimoto, W. Z. Zhang, S. Ishiwata, Y. Matsui, Y. Tokura, Near room-temperature formation of a skyrmion crystal in thin-films of the helimagnet FeGe. *Nat. Mater.* **10**, 106–109 (2011).
17. H. S. Park, X. Yu, S. Aizawa, T. Tanigaki, T. Akashi, Y. Takahashi, T. Matsuda, N. Kanazawa, Y. Onose, D. Shindo, A. Tonomura, Y. Tokura, Observation of the magnetic flux and three-dimensional structure of skyrmion lattices by electron holography. *Nat. Nanotechnol.* **9**, 337–342 (2014).
18. A. Bogdanov, A. Hubert, Thermodynamically stable magnetic vortex states in magnetic crystals. *J. Magn. Magn. Mater.* **138**, 255–269 (1994).
19. A. B. Butenko, A. A. Lenov, U. K. Rößler, A. N. Bogdanov, Stabilization of skyrmion textures by uniaxial distortions in noncentrosymmetric cubic helimagnets. *Phys. Rev. B* **82**, 052403 (2010).
20. M. N. Wilson, A. B. Butenko, A. N. Bogdanov, T. L. Monchesky, Chiral skyrmions in cubic helimagnet films: The role of uniaxial anisotropy. *Phys. Rev. B* **89**, 094411 (2014).
21. A. O. Leonov, T. L. Monchesky, N. Romming, A. Kubetzka, A. N. Bogdanov, R. Wiesendanger, The properties of isolated chiral skyrmions in thin magnetic films. *New J. Phys.* **18**, 065003 (2016).
22. I. E. Dzyaloshinskii, Theory of helicoical structures in antiferromagnets. I. Nonmetals. *Sov. Phys. JETP* **19**, 960 (1964).
23. H. Oike, A. Kikkawa, N. Kanazawa, Y. Taguchi, M. Kawasaki, Y. Tokura, F. Kagawa, Interplay between topological and thermodynamic stability in a metastable magnetic skyrmion lattice. *Nat. Phys.* **12**, 62–66 (2016).
24. A. Neubauer, C. Pfleiderer, B. Binz, A. Rosch, R. Ritz, P. G. Niklowitz, P. Böni, Topological Hall effect in the *A* phase of MnSi. *Phys. Rev. Lett.* **102**, 186602 (2009).
25. S.-Z. Lin, A. Saxena, C. D. Batista, Skyrmion fractionalization and merons in chiral magnets with easy-plane anisotropy. *Phys. Rev. B* **91**, 224407 (2015).
26. K. Karube, J. S. White, N. Reynolds, J. L. Gavilano, H. Oike, A. Kikkawa, F. Kagawa, Y. Tokunaga, H. M. Rønnow, Y. Tokura, Y. Taguchi, Robust metastable skyrmions and their triangular–square lattice structural transition in a high-temperature chiral magnet. *Nat. Mater.* **15**, 1237–1242 (2016).
27. C. Pfleiderer, D. Reznik, L. Pintschovius, H. V. Lohneysen, M. Garst, A. Rosch, Partial order in the non-Fermi-liquid phase of MnSi. *Nature* **427**, 227–231 (2004).
28. B. Binz, A. Vishwanath, V. Aji, Theory of the helical spin crystal: A candidate for the partially ordered state of MnSi. *Phys. Rev. Lett.* **96**, 207202 (2006).
29. S. Tewari, D. Belitz, T. R. Kirkpatrick, Blue quantum fog: Chiral condensation in quantum helimagnets. *Phys. Rev. Lett.* **96**, 047207 (2006).
30. V. Schweikhard, I. Coddington, P. Engels, S. Tung, E. A. Cornell, Vortex-lattice dynamics in rotating spinor Bose-Einstein condensates. *Phys. Rev. Lett.* **93**, 210403 (2004).
31. K. Kasamatsu, M. Tsubota, M. Ueda, Vortex phase diagram in rotating two-component Bose-Einstein condensates. *Phys. Rev. Lett.* **91**, 150406(2003).
32. F. Kagawa, H. Oike, Quenching of charge and spin degrees of freedom in condensed matter. *Adv. Mater.*, 10.1002/adma.201601979 (2016).

Acknowledgments: We thank G. Davidson and P. Imperia for technical support in the SANS experiment. We also thank K. Karube, Y. Tokunaga, X. Z. Yu, and D. Morikawa for enlightening discussions. **Funding:** This work was partly supported by the RIKEN Incentive Research Projects of and the Japan Society for the Promotion of Science Grants-in-Aid for Scientific Research (KAKENHI) (grants 25220709 and 15H05459). **Author contributions:** T.-h.A., F.K., K.K., and Y. Tokura conceived the project. T.N. and H.O. designed the experiments with discussions with E.P.G. and N.B. A.K. and Y. Taguchi grew the single crystals of MnSi used in the experiment. T.N., H.O., E.P.G., and N.B. performed the SANS and in situ resistivity measurements. T.N. wrote the manuscript with contributions from all the authors. **Competing interests:** The authors declare that they have no competing interests. **Data and materials availability:** All data needed to evaluate the conclusions in the paper are included in the paper and/or the Supplementary Materials. Additional data related to this paper may be requested from T.N. (taro.nakajima@riken.jp).

Submitted 19 October 2016
Accepted 13 April 2017
Published 9 June 2017
10.1126/sciadv.1602562

Citation: T. Nakajima, H. Oike, A. Kikkawa, E. P. Gilbert, N. Booth, K. Kakurai, Y. Taguchi, Y. Tokura, F. Kagawa, T.-h. Arima, Skyrmion lattice structural transition in MnSi. *Sci. Adv.* **3**, e1602562 (2017).

Science Advances

Skyrmion lattice structural transition in MnSi

Taro Nakajima, Hiroshi Oike, Akiko Kikkawa, Elliot P. Gilbert, Norman Booth, Kazuhisa Kakurai, Yasujiro Taguchi, Yoshinori Tokura, Fumitaka Kagawa and Taka-hisa Arima

Sci Adv **3** (6), e1602562.
DOI: 10.1126/sciadv.1602562